

Molecular-orbital studies via satellite-free x-ray fluorescence: Cl K absorption and K -valence-level emission spectra of chlorofluoromethanes

R. C. C. Perera

Advanced Light Source, Lawrence Berkeley Laboratory, Berkeley, California 94720

P. L. Cowan, D. W. Lindle, R. E. LaVilla, T. Jach, and R. D. Deslattes

Quantum Metrology Division, National Institute of Standards and Technology, Gaithersburg, Maryland 20899

(Received 21 September 1990)

X-ray absorption and emission measurements in the vicinity of the chlorine K edge of the three chlorofluoromethanes have been made using monochromatic synchrotron radiation as the source of excitation. By selectively tuning the incident radiation to just above the Cl $1s$ single-electron ionization threshold for each molecule, less complex x-ray-emission spectra are obtained. This reduction in complexity is attributed to the elimination of multielectron transitions in the Cl K shell, which commonly produce satellite features in x-ray emission. The resulting "satellite-free" x-ray-emission spectra exhibit peaks due only to electrons in valence molecular orbitals filling a single Cl $1s$ vacancy. These simplified emission spectra and the associated x-ray absorption spectra are modeled using straightforward procedures and compared with semiempirical ground-state molecular-orbital calculations. Good agreement is observed between the present experimental and theoretical results for valence-orbital energies and those obtained from ultraviolet photoemission, and between relative radiative yields determined both experimentally and theoretically in this work.

I. INTRODUCTION

The general quantitative application of x-ray spectroscopy to structural and dynamical studies of atoms and molecules has proved problematical because of the obscuring effect of multivacancy processes, which are usually present in addition to single-vacancy transitions in conventional x-ray spectra.¹ These multivacancy processes, in which two or more electrons are excited or ionized, result in extra features, termed satellites, in x-ray-absorption and -emission spectra. With the availability of tunable monochromatic x rays at synchrotron-radiation sources, it is now possible to selectively ionize core electrons near enough to the core-level threshold energy that multielectron transitions in the subshell of interest are energetically forbidden. Under these conditions, x-ray emission (fluorescence) is observed *only* from singly ionized atoms² or molecules, without contributions from multivacancy satellites: hence the term "satellite-free x-ray emission." Selective excitation, however, does not preclude the occurrence of multielectron transitions in the x-ray-emission process. But such transitions are expected to be very weak, in x-ray emission, unlike in the initial photoabsorption process, there is no change in charge state to cause "shake-up" or "shake-off" phenomena.

In this work, we present a study of the valence electronic structure of the chlorofluoromethanes by chlorine K x-ray emission under satellite-free conditions. We demonstrate how this technique, based on the use of synchrotron radiation, can eliminate multivacancy effects

that are inherent in conventional x-ray spectroscopy.¹ For this report, Cl K absorption spectra and Cl K - V emission spectra (K -valence-level, historically denoted as Cl $K\beta$) of gas-vapor phase CF_3Cl , CF_2Cl_2 , and CFCl_3 were measured using monochromatic synchrotron radiation from the National Institute of Standards and Technology (NIST) beamline X-24A at the National Synchrotron Light Source (NSLS) as the source of excitation. In order to estimate contributions from satellite features in the x-ray-emission spectra,^{2,3} Cl K - V fluorescence spectra were recorded for several incident x-ray energies in the vicinity of the single- and multiple-vacancy Cl K ionization thresholds. Appropriate photon energies for producing satellite-free spectra were selected, and single-vacancy Cl K emission spectra were recorded for all three samples. Comparison to previous core-level^{4,5} and valence-shell⁶⁻⁸ studies is made to assist in determining peak assignments. To further guide the interpretation of the satellite-free spectra, semiempirical ground-state modified neglect of diatomic-overlap (MNDO) calculations⁹ were performed for the valence molecular orbitals (MO's). In these calculations, the molecular geometry was varied to minimize the orbital energies, while retaining the proper ground-state molecular symmetry.¹⁰ Thus, the Cl K - V emission spectra have been analyzed by a method first described by Manne,¹¹ based upon atomic-orbital compositions of MO's.

We find that production of satellite-free x-ray-emission spectra is feasible, and that simplified spectra are indeed obtained using selective photon excitation. Comparison of the K - V emission data with MO binding energies from ul-

traviolet photoelectron spectroscopy (UPS) and with calculated relative yields provides adequate explanations of the observed spectra. With this demonstration it is suggested that satellite-free x-ray-emission measurements can be helpful in the assignment of MO's in more complex molecules. This latter possibility exists in part because x-ray emission involves only a subset of valence MO's with appreciable electron density at the site of the initially produced core hole.

II. EXPERIMENT

Detailed descriptions of the soft-x-ray beamline¹² and double-crystal monochromator¹³ are given elsewhere. Chlorine *K* absorption spectra are obtained by measuring incident and transmitted x-ray fluxes with ion chambers filled with a He-N₂ mixture at 1 atm. The Cl *K-V* fluorescence radiation is analyzed by a variable-radius curved-crystal¹⁴ spectrometer consisting of a silicon (111) crystal of $2d = 6.271 \text{ \AA}$ and a linear position-sensitive gas proportional counter¹⁵ filled with a Xe (90% vol)-CH₄ (10% vol) mixture at a pressure of ≈ 1 atm. The sample gas, contained in a 7-mm-long sample cell by 25- μm -thick beryllium windows, is located inside the Rowland circle of the secondary spectrometer. Further details of the spectrometer and its performance are given elsewhere.¹⁶

Energy calibration for the absorption spectra and the primary monochromator in this energy region was obtained using Cl *K* absorption spectra of the chlorofluoromethanes measured with a previously described¹⁷ laboratory spectrometer. Energy calibration of the emission spectra was obtained using positions of x-ray-emission features and elastically scattered x rays. The elastic peaks were observed with excitation at energies below all Cl *K* absorption features to avoid self-absorption effects. The x-ray emission data presented in this work were measured for emission polarized perpendicular to the incident radiation polarization.¹⁸ Observations to date indicate that fluorescence-polarization effects are generally small (<20%) for above-threshold excitation.^{19,20}

All samples were obtained commercially with stated purities greater than 99% and used without further purification. Sample gas pressures are selected empirically to correspond to approximately one absorption length (i.e., $I = I_0/e$) at the peak of absorption. For spectra presented in this work, the sample pressures for CF₃Cl, CF₂Cl₂, and CFCI₃ were 150, 100, and 60 Torr, respectively.

III. RESULTS AND DISCUSSION

One reason for studying the chlorofluoromethanes is the extensive body of results from previous studies employing a variety of techniques. For example, x-ray-absorption measurements of CF₂Cl₄ were made by Hanus and Gilberg.²¹ X-ray-excited Cl *K-V* emission spectra of CF₃Cl, CF₂Cl₂, and CFCI₃ were reported previously by LaVilla and Deslattes,⁴ while Ehlert and Mattson⁵ measured F *K*, C *K*, and Cl *L*_{II,III} emission spectra. Ultraviolet photoelectron spectra of the chlorofluoromethanes have been measured by Doucet, Sauvageau, and Sandorfy⁶ and

Jadrny *et al.*⁷ using He I (21.2 eV) excitation. Cvitas, Gusten, and Klasinc⁸ confirmed and extended the UPS measurements with He I and He II (40.8-eV) radiation. All of the experimental photoelectron spectra are in good agreement.

For analyzing the present absorption spectra, a theoretical model suggested by Wainstein, Barinskij, and Narbutt²² was used. The shape of an absorption spectrum is assumed to be determined mainly by the positive-charge core hole, with molecular effects reflected in the first one or two discrete (below-threshold) absorption features. An atomiclike Rydberg series is used to account for the absorption just below the *K*-shell threshold. Finally, the absorption continuum is described by an arctangent function such that the point of inflection coincides with the ionization threshold of the Cl 1*s* core level. Based upon these assumptions, the absorption spectra were decomposed into Voigt spectra components²³ to account for single-electron transitions to unoccupied valence MO's, a Rydberg series leading to the Cl *K* threshold, and an absorption continuum described by an arctangent function. The quantum defects²⁴ for the components of the Rydberg series were assumed to be the same, and the area encompassed by the entire Rydberg series depends upon the absorption coefficient in the continuum²² (i.e., the maximum height of the arctangent function). For the modeling procedures in this work,²⁴ Rydberg series of $n = 5$ to 25 were used. No attempt was made to model any of the above-threshold features in the chlorofluoromethane absorption spectra. Previously, Hanus and Gilberg²¹ successfully used a similar procedure to describe Cl *K* core-level absorption measurements.

To facilitate interpretation of the experimental features in the present x-ray-emission spectra, the spectra were modeled empirically using a SIMPLEX minimization technique.²³ For the modeling, the instrumental broadening was assumed to Gaussian and the natural linewidth Lorentzian, resulting in Voigt spectral profiles. The Gaussian instrumental broadening was estimated to be 1.0 eV by analyzing a series of x-ray-emission spectra in this region. This value is consistent with direct measurements of the secondary-spectrometer resolution.

Modeling of the x-ray-emission spectra permitted extraction of energies and relative intensities of the emission peaks. Assignments were then determined by comparison with known valence MO orderings from UPS measurements.⁶⁻⁸ MNDO calculations⁹ also were compared to the observed spectra and their assignments, in particular to identify those valence MO's with appreciable Cl 3*p* atomic-orbital character.¹¹ Only MO's with some Cl 3*p* character will contribute to the x-ray-emission spectra. Finally, the MNDO calculations provided relative intensities in good agreement with observation, leading further confidence to the present assignments.²⁵

A. Trifluorochloromethane (CF₃Cl)

Trifluorochloromethane (C_{3v} symmetry point group) has 32 valence electrons in the ground-state electronic configuration

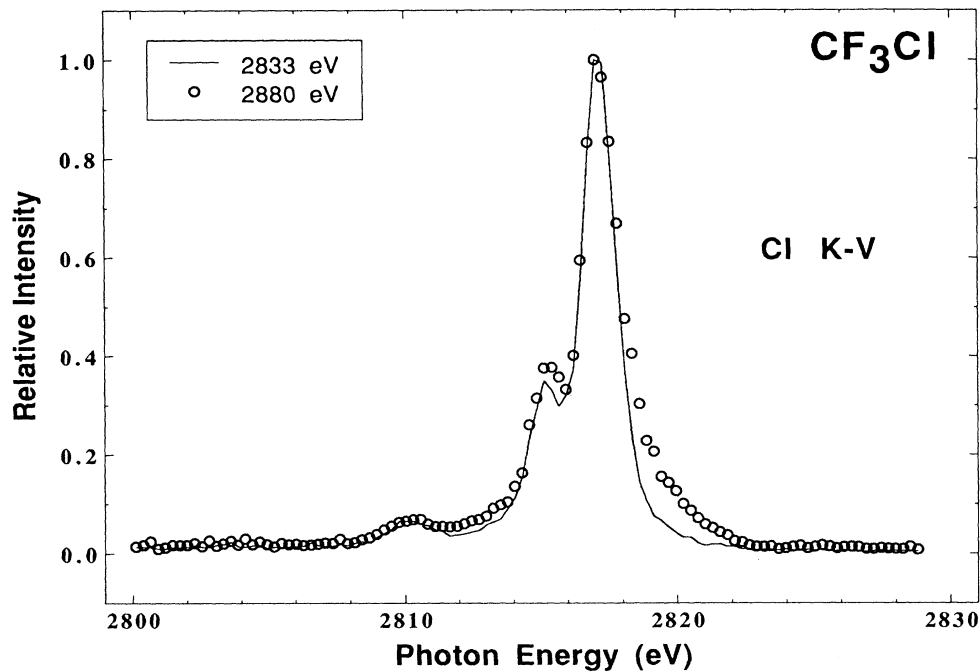


FIG. 1. Comparison of 2880-eV photon-energy-excited Cl K - V spectrum of CF_3Cl (circles) with a 2833-eV excited spectrum indicated by the solid curve. The increased intensity contributions in the 2880-eV excited spectrum are attributed to multiple-vacancy transitions.

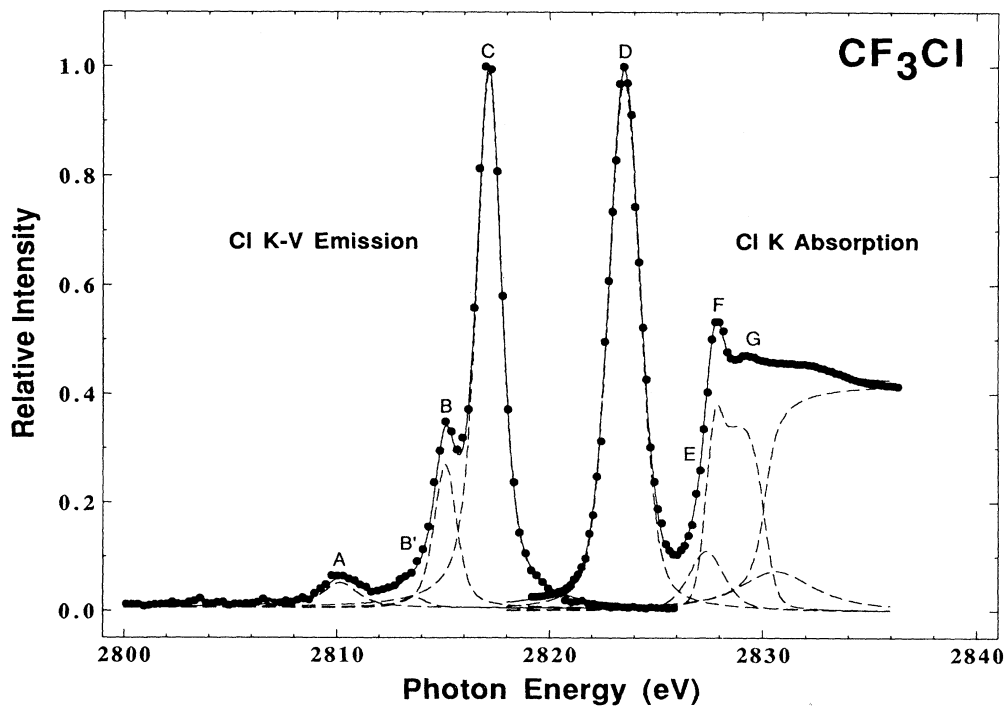


FIG. 2. Experimental 2833-eV photon-energy-excited Cl K - V emission and K absorption spectra of CF_3Cl (dots) along with fitted spectral components (dashed curves) and the sum of the derived components (solid curves). The component energies and assignments are given in Table I.

TABLE I. Energies, relative radiation yields, and assignments for the major components in the Cl *K* absorption and Cl *K-V* emission spectra of CF₃Cl, CF₂Cl₂, and CFCI₃.

Peak	CF ₃ Cl			CF ₂ Cl			CFCI ₃		
	Energy (eV)	Relative Intensity	Assignment	Energy (eV)	Relative Intensity	Assignment	Energy (eV)	Relative Intensity	Assignment
Emission									
<i>A</i>	2810.1(3)	5	9 <i>a</i> ₁ + 4 <i>e</i>	2810.4(3)	13	3 <i>b</i> ₁ + 10 <i>a</i> ₁ + 7 <i>b</i> ₂	2811.5(4)	19	7 <i>e</i>
<i>B'</i>	2813.6(3)	2	5 <i>e</i>						
<i>B</i>	2815.1(3)	27	10 <i>a</i> ₁	2813.1(5)	17	2 <i>a</i> ₂ + 11 <i>a</i> ₁	2814.4(5)	22	8 <i>e</i>
<i>C'</i>				2815.8(3)	48	12 <i>a</i> ₁ + 8 <i>b</i> ₂	2816.3(3)	88	9 <i>e</i> + 11 <i>a</i> ₁
<i>C</i>	2817.1(3)	100	7 <i>e</i>	2817.0(3)	100	9 <i>b</i> ₂ + 5 <i>b</i> ₁ + 3 <i>a</i> ₂	2817.4(3)	100	2 <i>a</i> ₂ + 10 <i>e</i>
Absorption									
<i>D</i>	2823.5 ^a		Cl 1 <i>s</i> → 11 <i>a</i> ₁	2823.0 ^a		Cl 1 <i>s</i> → 13 <i>a</i> ₁ + 10 <i>b</i> ₂	2822.8 ^a		Cl 1 <i>s</i> → 12 <i>a</i> ₁
<i>E</i>	2827.4(3)		Cl 1 <i>s</i> → 12 <i>a</i> ₁ + 8 <i>e</i>	2826.4(3)		Cl 1 <i>s</i> → 14 <i>a</i> ₁ + 6 <i>b</i> ₁	2825.7(5)		Cl 1 <i>s</i> → 11 <i>e</i> + 13 <i>a</i> ₁
<i>F</i>	2827.8(3)		Cl 1 <i>s</i> → 4 <i>p</i>	2827.2(3)		Cl 1 <i>s</i> → 4 <i>p</i>	2827.1(3)		Cl 1 <i>s</i> → 4 <i>p</i> ···
<i>IP</i>	2830.2 ^b (3)		Cl 1 <i>s</i> → ∞	2829.6 ^b (6)		Cl 1 <i>s</i> → ∞	2829.3 ^b (5)		Cl 1 <i>s</i> → ∞
	2830.13 ^c			2829.60 ^c			2829.30 ^c		

^aPeaks used in calibration of absorption spectra.^bFrom UPS and Cl *K-V*.^cFrom Rydberg peaks (this work).TABLE II. Results from ground-state semiempirical MNDO calculations for CF₃Cl.

Assignment	Orbital composition					
	Carbon		Fluorine		Chlorine	
	2 <i>s</i>	2 <i>p</i>	2 <i>s</i>	2 <i>p</i>	3 <i>s</i>	3 <i>p</i>
7 <i>e</i>				0.047		1.953
10 <i>a</i> ₁	0.006	0.066		0.587	0.006	0.335
6 <i>e</i>		0.018	0.008	1.974		
1 <i>a</i> ₂				1.000		
5 <i>e</i>		0.002	0.001	1.984		0.013
4 <i>e</i>		0.419	0.194	1.366		0.022
9 <i>a</i> ₁	0.001	0.259	0.022	0.549	0.040	0.129
8 <i>a</i> ₁	0.203	0.001	0.199	0.294	0.254	0.050
7 <i>a</i> ₁	0.092	0.049	0.066	0.051	0.695	0.046
3 <i>e</i>		0.255	1.698	0.045		0.002
6 <i>a</i> ₁	0.269	0.020	0.650	0.054	0.001	0.007

TABLE III. Comparison of experimental and calculated orbital energies and Cl *K-V* relative intensities for CF₃Cl.

Peak	Orbital	Energy (eV)		Relative intensity	
		UPS ^a	Calculated	Experimental	Calculated
<i>C</i>	7 <i>e</i>	13.08	14.1	100	100
<i>B</i>	10 <i>a</i> ₁	15.20	15.2	27	17
	1 <i>a</i> ₂	15.80	17.0		0
	6 <i>e</i>	16.72	16.8		0
<i>B'</i>	5 <i>e</i>	17.71	17.3	2	1
<i>A</i>	9 <i>a</i> ₁	20.20	20.9		5
	4 <i>e</i>	21.2	20.8	1	
	8 <i>a</i> ₁	23.8	24.6	3	
	7 <i>a</i> ₁		27.4	2	
	3 <i>e</i>		45.4	0	
	6 <i>a</i> ₁		52.3	0	

^aReferences 6–8.

$$(6a_1)^2(3e)^4(7a_1)^2(8a_1)^2(9a_1)^2(4e)^4(5e)^4(1a_2)^2(6e)^4(10a_1)^2(7e)^4.$$

The first occupied valence MO's, based on MNDO calculations, are $11a_1$, $12a_1$, and $8e$ in order of increasing energy.

Using our Cl K - V x-ray-emission data and UPS final-state binding energies (BE),^{7,8} the Cl $1s$ ionization threshold of CF_3Cl is estimated to be 2830.2(3) eV, compared to 2830.13 eV from the Rydberg peak positions in this work. The Cl K - V emission spectra presented in Fig. 1 were obtained using photon excitation energies of 2833 and 2880 eV. The lower photon energy is about 3 eV above the Cl $1s$ ionization threshold, and below all double-vacancy thresholds, resulting in a satellite-free Cl K - V spectrum. A photon energy of 2880 eV is above most [K V] double-vacancy threshold energies, which correspond to production of initial states that make important contributions to emission satellites in this energy range. As seen in Fig. 1, the 2880-eV spectrum (dots) contains extra contributions which we attribute to multiple-vacancy transitions. The main satellite emission band thus obtained is located on the high-energy side of the single-vacancy spectrum. The primary concern for the present work is that the multiple-vacancy emission features can be suppressed by selectively tuning the excitation energy, as was demonstrated originally for Ar K -edge x-ray-emission spectra.²

The 2833-eV Cl K - V spectrum is presented again in Fig. 2, along with modeled Voigt spectral components and their sum. Listed in Table I are energies of the Voigt components and their relative areas, which are propor-

tional to relative radiative yields. The Cl K absorption spectrum of CF_3Cl is shown in Fig. 2, along with the fit results. The energy positions and relative intensities for the discrete Cl K absorption features of CF_3Cl also are given in Table I. As indicated earlier, no attempt was made to model the features above the ionization threshold; hence, no quantitative results will be reported for this feature at 2830 eV.

The lowest-energy absorption feature in the Cl K region of CF_3Cl , labeled D in Fig. 2, is assigned to a transition of a Cl $1s$ electron to the unoccupied $11a_1$ valence MO. The small-amplitude feature E at 2826.5 eV may be derived from transitions to the $12a_1$ or $8e$ valence MO's. As seen for the derived components in Fig. 2, feature F results from transitions to the $4p$ Rydberg state, whereas feature G is attributed to overlapping transitions to $5p$ and higher Rydberg states leading to the Cl $1s$ ionization threshold. These assignments are summarized in Table I. The broad structure above the $1s$ threshold is tentatively attributed to a shape-resonance structure. Similar suprathreshold structures were observed and identified³ in Cl K emission and absorption spectra of CH_3Cl .

Because of selective excitation of CF_3Cl at 2833 eV, all emission features in the Cl K - V spectrum in Fig. 2 have a common initial state, namely, a single Cl $1s$ vacancy. Thus, the most probable transitions in the K - V emission spectrum involve electrons from valence MO's with Cl $3p$ character.¹¹ A reasonable estimate of the chlorine $3p$

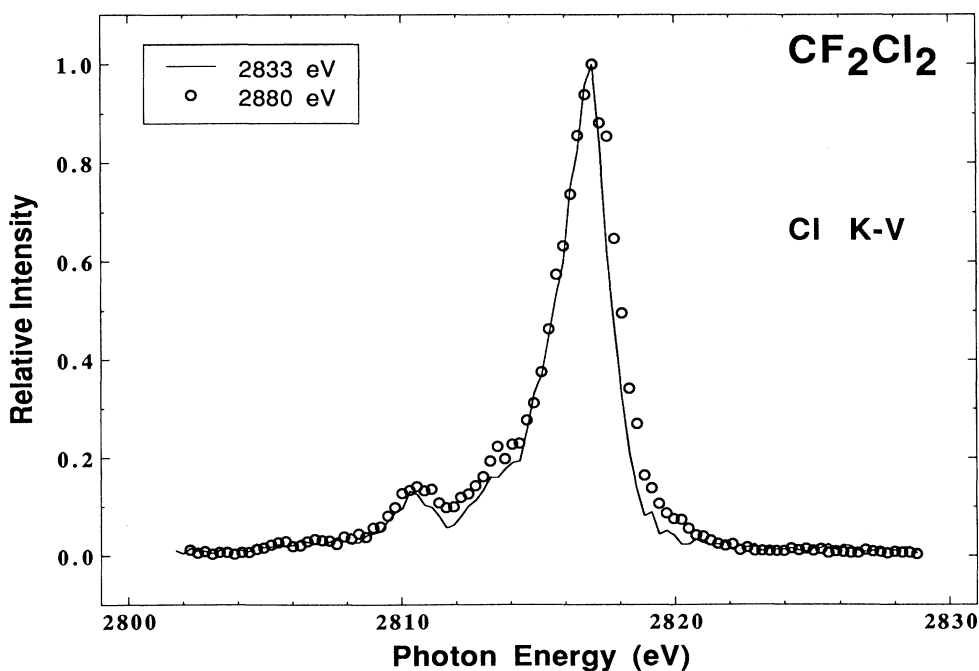


FIG. 3. Cl K - V emission spectra from CF_2Cl_2 using 2880 (circles) and 2833-eV (solid curve) photon-energy excitation.

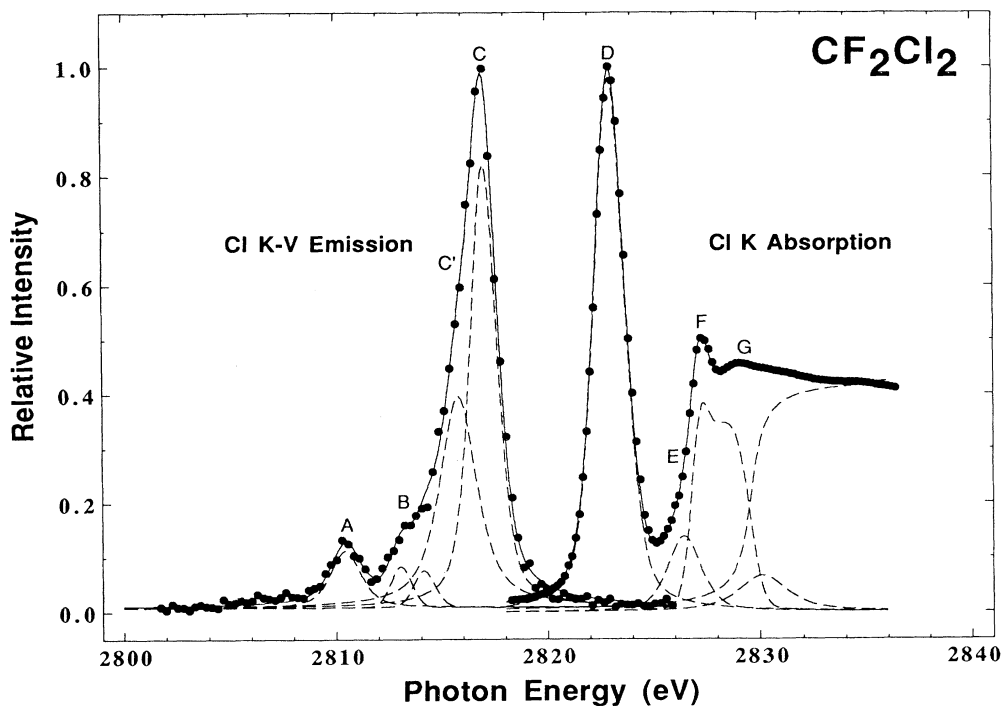


FIG. 4. The 2833-eV excited Cl *K-V* emission and *K* absorption spectra of CF_2Cl_2 , as in Fig. 2.

character in a valence MO can be obtained from a simple ground-state calculation, such as MNDO, as shown in Ref. 10. Therefore, we have calculated energies and compositions for the valence MO's of CF_3Cl by the MNDO method, and the results are listed in Table II. Atomic-orbital compositions can be obtained from the squared coefficients for each contributing atomic orbital to the CF_3Cl molecular orbitals.

Comparison of the observed CF_3Cl *K-V* emission features with calculated energies and intensities is shown

in Table III. The stronger emission components, peaks *C* and *B*, are assigned to dipole-allowed transitions of electrons in the $7e$ and $10a_1$ valence MO's, respectively, filling the initial Cl $1s$ vacancy. The weaker emission peaks *B'* and *A* are assigned to allowed dipole transitions from the $5e$ and the $9a_1 + 4e$ valence MO's, respectively. As seen from Table III, experimental values agree reasonably well with the calculated radiative yields based upon ground-state calculations. The experimental binding energies are only in fair agreement since the ordering of

TABLE IV. Results from ground-state semiempirical MNDO calculations for CF_2Cl_2 .

Assignment	Carbon		Orbital Composition Fluorine		Chlorine	
	2s	2p	2s	2p	3s	3p
$9b_2$		0.016		0.010	0.001	0.973
$3a_2$				0.010		0.990
$5b_1$				0.039		0.961
$12a_1$	0.002	0.005		0.043		0.950
$8b_2$		0.084		0.410	0.005	0.500
$11a_1$	0.004	0.038	0.002	0.782	0.004	0.171
$4b_1$		0.005	0.002	0.992		0.001
$2a_2$				0.990		0.010
$7b_2$		0.262		0.517	0.040	0.180
$3b_1$		0.209	0.095	0.669		0.026
$10a_1$	0.002	0.243	0.040	0.540	0.030	0.144
$9a_1$	0.152		0.109	0.156	0.507	0.076
$6b_2$		0.035		0.006	0.948	0.010
$8a_1$	0.215	0.054	0.113	0.056	0.451	0.112
$2b_1$		0.127	0.851	0.021		0.002
$7a_1$	0.223	0.042	0.675	0.045	0.001	0.014

TABLE V. Comparison of experimental and calculated orbital energies and Cl K - V relative intensities for CF_2Cl_2 .

Peak	Orbital	Energy (eV)		Relative intensity	
		UPS ^a	Calculated	Experimental	Calculated
C	$9b_2$	12.25	13.4	100	33
	$5b_1$	12.53	14.2		33
	$3a_2$	13.11	13.9		34
	$12a_1$	13.45	14.3		33
C'	$8b_2$	14.36	14.8	48	17
	$4b_1$	15.9	16.9		0
	$2a_2$	16.3	17.2		8
B	$11a_1$	16.9	16.5	9	6
	$3b_1$	19.5	20.4		1
	$10a_1$	19.5	20.5		13
A	$7b_2$	20.4	20.4	13	6
	$9a_1$	22.5	24.7		3
	$6b_2$		26.6		<1
	$8a_1$		28.4		4
	$2b_1$		45.4		0
	$7a_1$		50.7		<1

^aReferences 6–8.

valence MO's suggested by the MNDO method interchanges the $1a_2$ and $6e$, and the $9a_1$ and $4e$ valence MO's. This shortcoming to the MNDO calculation is expected because the method treats the MO's as combinations of atomic orbitals, with little detailed optimization of the MO energies. Therefore, we stress that our assignments are based primarily on energetic grounds using UPS binding-energy measurements. The MNDO results are used only to determine which MO's have appreciable

Cl $3p$ atomic-orbital character, and for a rough comparison with the observed emission intensities.

B. Dichlorodifluoromethane (CF_2Cl_2)

Dichlorodifluoromethane (C_{2v} point group) also has 32 valence electrons which are distributed among 16 different valence molecular orbitals. The ground-state valence electronic configuration is

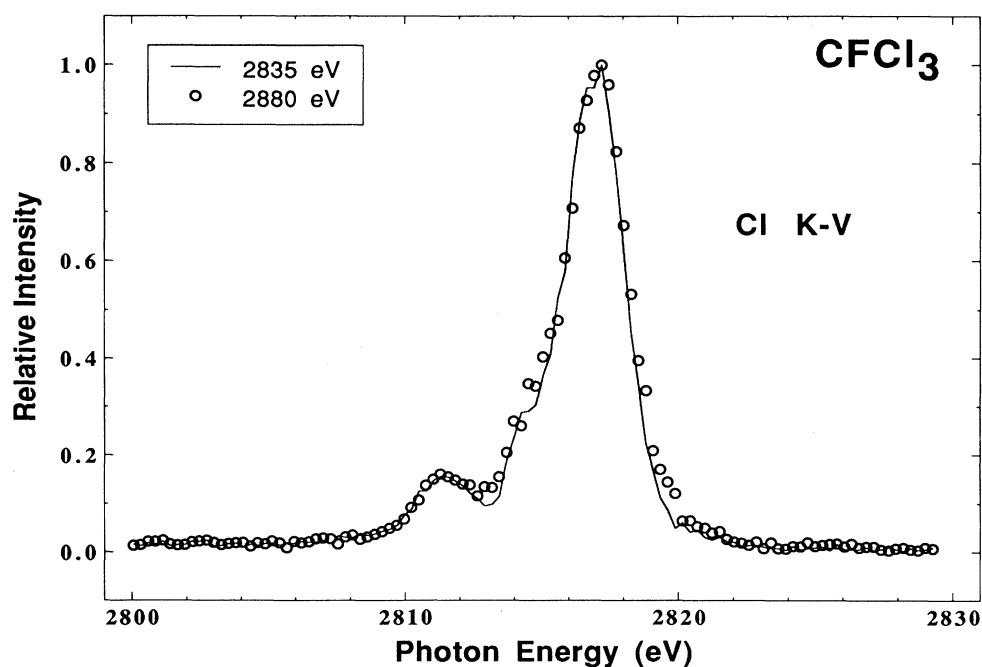


FIG. 5. Cl K - V emission spectra of CFCl_2 using 2835 (solid curve) and 2880-eV (circles) photon-energy excitation.

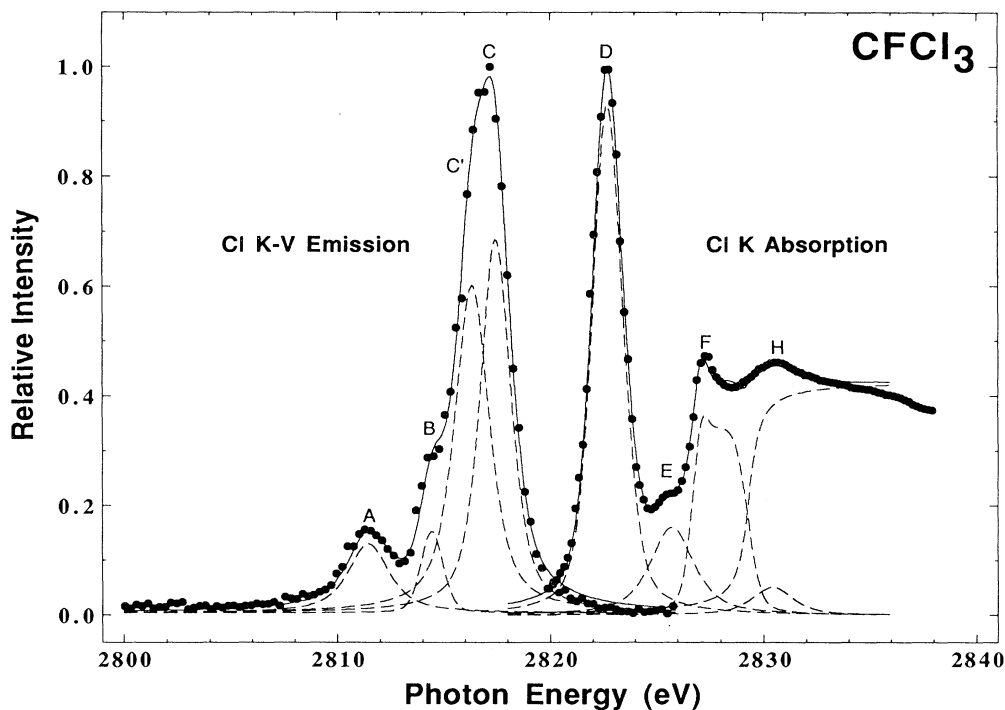


FIG. 6. The 2835-eV excited Cl *K-V* emission and *K* absorption spectra of CFCl_3 , as in Fig. 2.

$$(7a_1)^2(2b_1)^2(8a_1)^2(6b_2)^2(9a_1)^2(7b_2)^2(10a_1)^2(3b_1)^2(11a_1)^2(2a_2)^2(4b_1)^2(8b_2)^2(12a_1)^2(3a_2)^2(5b_1)^2(9b_2)^2 .$$

The lowest unoccupied valence MO's of CF_2Cl_2 , based on MNDO calculations, are $13a_1$, $10b_2$, $14a_1$, and $6b_1$ in order of increasing energy.

The Cl *K-V* emission spectra from CF_2Cl_2 using 2833 and 2880 eV photon-energy excitation are presented in Fig. 3 for comparison. As in CF_3Cl , increased intensity contributions for 2880-eV excitation visible in Fig. 3 are attributed to multiple-vacancy transitions. The satellite-free Cl *K-V* x-ray-emission spectrum of CF_2Cl_2 also is presented in Fig. 4, along with the derived Voigt spectral components. The energies and relative intensities of the prominent spectral features are listed in Table I.

The Cl *K* absorption spectrum of CF_2Cl_2 is shown in Fig. 4 along with the model components. The component energies, relative intensities, and their assignments are listed in Table I. The first discrete absorption maximum (feature *D*) and feature *E* are assigned to dipole-allowed transitions of the ground-state chlorine *1s* electron to the unoccupied $13a_1$ and $10b_2$, and the $14a_1$ and $6b_1$ valence MO's, respectively. As seen from the derived components in Fig. 4, features *F* and *G* result from overlapping of transitions to $4p$, $5p$, and higher Rydberg states leading to the chlorine *1s* ionization threshold. The broad structure above the *1s* threshold is tentatively attributed to a shape-resonance structure. These results for Cl *K* absorption of CF_2Cl_2 are consistent with previous lower-resolution measurements.²¹

For the Cl *K-V* emission spectrum of CF_2Cl_2 , the calculated orbital compositions and relative radiative yields are presented in Table IV. The results in Table IV suggest that the strongest feature *C* in Fig. 4 results from overlapping, dipole-allowed, transitions from the $9b_2$, $5b_1$, and $3a_2$ valence MO's, whereas feature *C'* is assigned to transitions from the $12a_1$ and $8b_2$ valence MO's. The broad feature *B*, (corresponding to two derived components) is assigned to transitions from the $2a_2$ and $11a_1$ orbitals, whereas the feature *A* is assigned to transitions from the $3b_1$, $10a_1$, and $7b_2$ valence MO's. Very weak features resulting from transitions that originate from inner-valence $8a_1$ and $9a_1$ MO's are perhaps present near 2806 eV. These assignments are summarized in Table I.

The calculated and experimental valence MO energies and Cl *K-V* relative radiative yields for CF_2Cl_2 are compared in Table V. The ordering of valence MO's suggested by the MNDO method does not agree with the assignment of the UPS spectra. However, the relative intensities are in good agreement, after putting the MNDO results in the correct order.

C. Trichlorofluoromethane (CFCl_3)

Trichlorofluoromethane (C_{3v} symmetry) has a ground-state valence configuration of

TABLE VI. Results from ground-state semiempirical MNDO calculations for CFCl₃.

Assignment	Orbital composition					
	Carbon		Fluorine		Chlorine	
	2s	2p	2s	2p	3s	3p
2a ₂						1.000
10e		0.049		0.012	0.002	1.938
9e		0.032		0.079	0.002	1.888
11a ₁	0.002	0.002		0.052		0.943
8e		0.149		0.926	0.011	0.915
7e		0.507		0.920	0.072	0.501
10a ₁	0.002	0.243	0.067	0.512	0.019	0.157
9a ₁	0.109		0.044	0.062	0.694	0.090
6e		0.070		0.007	1.902	0.021
8a ₁	0.350	0.045	0.110	0.028	0.278	0.189
7a ₁	0.155	0.071	0.721	0.034	0.002	0.018

$$(7a_1)^2(8a_1)^2(6e)^4(9a_1)^2(10a_1)^2(7e)^4(8e)^4(11a_1)^2(9e)^4(10e)^4(2a_2)^2.$$

From the MNDO calculations, the lowest unoccupied valence MO's are 12a₁, 11e, and 13a₁ in order of increasing energy. Chlorine *K-V* x-ray-emission spectra of CFCl₃ in the vapor phase were measured using 2835- and 2880-eV excitation, and are presented in Fig. 5 for comparison. Note the increase in intensity resulting from multiple-vacancy transitions. However, their contributions appear less prominent than in CF₃Cl or CF₂Cl₂.

A satellite-free Cl *K-V* x-ray-emission spectrum of CFCl₃ is presented in Fig. 6 along with the modeled Voigt spectral components. The component energies and relative intensities of the spectral features are listed in Table I. The orbital compositions and Cl *K-V* radiative yields suggested by the ground-state MNDO MO calculations are presented in Table VI.

The Cl *K* absorption spectrum of CFCl₃ also is shown in Fig. 6 along with its modeled components. The energies, relative intensities, and their assignments are presented in Table I. Feature *D*, the first discrete max-

imum in the absorption spectrum, is assigned to the dipole-allowed transition of a chlorine 1s electron to the unoccupied valence 12a₁ MO, whereas feature *E* is attributed to transitions to the 11e and 13a₁ unoccupied valence MO's. Again, feature *F* results from 4p and higher Rydberg states, and it is suggested that the broad feature *H* might be a shape resonance.

For the Cl *K-V* emission spectrum, the main features, *C* and *C'*, are assigned to dipole-allowed overlapping transitions from the 2a₂ and 10e, and the 9e and 11a₁ valence MO's, respectively, whereas the weak feature *B* is assigned to a transition from the 8e valence MO. The prominent peak *A* is assigned to a transition from the 7e valence MO.²⁰ These assignments are listed in Table I. As seen from Table VII the calculated and experimental valence MO energies and Cl *K-V* relative radiative yields for CFCl₃ are in fair agreement. Also the ordering of valence MO's suggested by the MNDO method is the same as the assignment of the UPS spectra.

TABLE VII. Comparison of experimental and calculated orbital energies and Cl *K-V* relative intensities for CFCl₃.

Peak	Orbital	Energy (eV)		Relative intensity	
		UPS ^a	Calculated	Experimental	Calculated
<i>C</i>	2a ₂	11.73	13.3	100	34
	10e	12.13	13.4		66
<i>C'</i>	9e	12.97	14.1	88	64
	11a ₁	13.45	14.3		32
<i>B</i>	8e	15.05	15.8	22	31
<i>A</i>	7e	18.2	19.7	19	17
	10a ₁	18.2	19.9		5
	9a ₁	21.5	24.7		3
	6e		26.5		1
	8a ₁		30.2		7
	7a ₁		48.7		1

^aReferences 6-8.

IV. CONCLUSION

We have demonstrated the feasibility of producing gas-phase molecular x-ray-emission spectra free of the complicating influences of multielectron (multivacancy satellite) effects. These so-called "satellite-free" spectra can be interpreted adequately using relatively simple theoretical models, giving insight into the assignments and relative yields for the observed valence-molecular-orbital x-ray transitions. Such simplified x-ray-emission spectra may be particularly useful for more complex molecules, where the advantages of the propensity to follow atomic dipole selection rules (e.g., Cl $3p \rightarrow 1s$) will be most profound.

ACKNOWLEDGMENTS

We thank Barry Karlin for assisting in the measurements, and Dana Berkeland and Mark Thomas for their invaluable assistance in analyzing data. One of the authors (R.C.C.P.) acknowledges the support by the Director, Office of Energy Research, Office of Basic Energy Sciences, Materials Sciences Division, of the U.S. Department of Energy under the Contract No. DE-AC03-76SF00098. This work was performed at NSLS, which is supported by the U.S. Department of Energy under Contract No. DE-AC020-76CH00016.

- ¹R. D. Deslattes, *Aust. J. Phys.* **39**, 845 (1986) and references therein.
- ²R. D. Deslattes, R. E. LaVilla, P. L. Cowan, and A. Henins, *Phys. Rev. A* **27**, 923 (1983).
- ³R. C. C. Perera, J. Barth, R. E. LaVilla, R. D. Deslattes, and A. Henins, *Phys. Rev. A* **32**, 1489 (1985).
- ⁴R. E. LaVilla and R. D. Deslattes, *J. Chem. Phys.* **45**, 3446 (1966).
- ⁵R. C. Ehlert and R. A. Mattson, *J. Chem. Phys.* **48**, 5471 (1968).
- ⁶J. Doucet, P. Sauvageau, and C. Sandorfy, *J. Chem. Phys.* **58**, 3708 (1973).
- ⁷R. Jadrny, L. Karlsson, L. Mattson, and K. Siegbahn, *Phys. Scr.* **16**, 235 (1977).
- ⁸T. Cvitas, H. Gusten, and L. Klasinc, *J. Chem. Phys.* **67**, 2687 (1977).
- ⁹M. J. S. Dewar and G. P. Ford, *J. Am. Chem. Soc.* **101**, 5558 (1979).
- ¹⁰R. C. C. Perera and R. E. LaVilla, *J. Chem. Phys.* **84**, 4228 (1986).
- ¹¹R. Manne, *J. Chem. Phys.* **52**, 5733 (1970).
- ¹²P. L. Cowan, S. Brennan, R. D. Deslattes, A. Henins, T. Jach, and E. G. Kessler, *Nucl. Instrum. Methods A* **246**, 154 (1986); P. L. Cowan, S. Brennan, T. Jach, D. W. Lindle, and B. A. Karlin, *Rev. Sci. Instrum.* **60**, 1603 (1989).
- ¹³P. L. Cowan, J. B. Hastings, T. Jach, and J. P. Kirkland, *Nucl. Instrum. Methods* **208**, 349 (1983).
- ¹⁴A. Henins, *Rev. Sci. Instrum.* **58**, 1173 (1987).
- ¹⁵B. P. Duval, J. Barth, R. D. Deslattes, A. Henins, and G. G. Luther, *Nucl. Instrum. Methods* **222**, 274 (1984).
- ¹⁶S. Brennan, P. L. Cowan, R. D. Deslattes, A. Henins, D. W. Lindle, and B. A. Karlin, *Rev. Sci. Instrum.* **60**, 2243 (1989).
- ¹⁷R. D. Deslattes, *Rev. Sci. Instrum.* **38**, 616 (1967).
- ¹⁸D. W. Lindle, P. L. Cowan, R. E. LaVilla, T. Jach, R. D. Deslattes, B. Karlin, J. A. Sheehy, T. J. Gil, and P. W. Langhoff, *Phys. Rev. Lett.* **60**, 1010 (1988).
- ¹⁹D. W. Lindle, P. L. Cowan, T. Jach, R. E. LaVilla, and R. D. Deslattes, *Nucl. Instrum. Methods B* **40/41**, 257 (1989).
- ²⁰D. W. Lindle, P. L. Cowan, T. Jach, R. E. LaVilla, R. D. Deslattes, and R. C. C. Perera, *Phys. Rev. A* **43**, 2353 (1991).
- ²¹M. J. Hanus and E. Gilberg, *J. Phys. B* **9**, 137 (1976).
- ²²E. J. Wainstein, R. L. Barinskij, and K. I. Narbutt, *Dokl. Akad. Nauk. Fiz.* **77**, 1002 (1951); **78**, 39 (1951).
- ²³B. L. Henke, R. C. C. Perera, E. M. Gullikson, and M. L. Schattenburg, *J. Appl. Phys.* **49**, 480 (1978).
- ²⁴The energy of the n th Rydberg peak from the ionization threshold energy $\Delta E \propto 1/(n-q)^2$, where q is the quantum defect. For the modeling procedure in this work, Rydberg series of $n = 5, 25$ were used. The resulting quantum defects from this procedure for CF_3Cl , CF_2Cl_2 , and CFCl_3 are 0.70, 0.72, and 0.66, respectively.
- ²⁵[Additional information also can be obtained using polarized x-ray-emission spectroscopy (PXES) (Refs. 18 and 19). A case in point (Ref. 20) is emission peak *A* for CFCl_3 , where PXES results strongly indicate assignment to only the $2e$ MO, although the $4a_1$ MO is energetically possible as well. This result will be discussed in more detail in Ref. 20].